Original Article

Adsorption behavior of platinum-group metals and Co-existing metal ions from simulated high-level liquid waste using HONTA and Crea impregnated adsorbent

Naoki Osawa [a,b], Seong-Yun Kim [a,*], Masahiko Kubota [a], Hao Wu [a], Sou Watanabe [c], Tatsuya Ito [c], Ryuji Nagaishi [c]

[a] *Department of Quantum Science and Energy Engineering, Graduate School of Engineering, Tohoku University, Sendai, Miyagi, 980-8579, Japan*
[b] *Japan Nuclear Fuel Limited, Rokkasho, Kamikita, Aomori, 039-3212, Japan*
[c] *Japan Atomic Energy Agency, Tokai, Naka, Ibaraki, 319-1195, Japan*

ABSTRACT

The volume and toxicity of radioactive waste can be decreased by separating the components of high-level liquid waste according to their properties. An impregnated silica-based adsorbent was prepared in this study by combining N,N,N',N',N'',N''-hexa-n-octylnitrilotriacetamide (HONTA) extractant, N',N'-di-n-hexyl-thio-diglycolamide (Crea) extractant, and macroporous silica polymer composite particles (SiO_2–P). The performance of platinum-group metals adsorption and separation on prepared (HONTA + Crea)/SiO_2–P adsorbent was then assessed together with that of co-existing metal ions by batch-adsorption and chromatographic separation studies. From the batch-adsorption experiment results, (HONTA + Crea)/SiO_2–P adsorbent showed high adsorption performance of Pd(II) owing to an affinity between Pd(II) and Crea extractant based on the Hard and Soft Acids and Bases theory. Additionally, significant adsorption performance was observed toward Zr(IV) and Mo(VI). Compared with studies using the Crea extractant, the high adsorption performance of Zr(IV) and Mo(VI) is attributed to the HONTA extractant. As revealed from the chromatographic experiment results, most of Pd(II) was recovered from the feed solution using 0.2 M thiourea in 0.1 M HNO_3. Additionally, the possibility of recovery of Zr(IV), Mo(VI), and Re(VII) was observed using the (HONTA + Crea)/SiO_2–P adsorbent.

1. Introduction

Spent fuel generated by nuclear power generation contains various elements produced by nuclear fission reaction [1]. Uranium and plutonium are recovered from spent fuel by the PUREX method at the reprocessing plant. However, most elements, such as alkali metals, alkaline earth metals, transition metals, lanthanides, and actinides, are not recovered using the PUREX process and will be vitrified as high-level liquid waste (HLLW) for geological disposal due to their radiation toxicity [2]. Particularly, platinum-group elements of the transition metals are known to interfere with the vitrification process by depositing within the vitrification melting furnace [3]. Numerous investigations on nuclide separation have been conducted using solvent extraction, precipitation, ion exchange, extraction chromatography etc. since separating these elements from HLLW will result in less hazardous waste, less volume, and even create scarce resources [4]. The solvent extraction

method, represented by the PUREX method, is a proven method in the nuclear power industry, and the development of extractants with different extraction characteristics is also progressing [5]. However, studies on the extraction chromatography using adsorbent in which an extractant is impregnated into macroporous silica polymer composite particles (SiO_2–P) are also conducted because the amount of harmful organic solvent used is small, the separation operation is simple solid–liquid separation, and the device configuration is compact [6]. Since the adsorption performance of the adsorbent is exhibited by the extractant impregnated into SiO_2–P, the knowledge of the solvent extraction method can be used.

It was shown that the Hard and Soft Acids and Bases (HSAB) theory is effective for palladium adsorption. Therefore, adsorbents using thio-diglycolamide (TDGA)-type extractants, such as N,N'-dimethyl-N,N'-di-n-octyl-thiodiglycolamide (MOTDGA), $N,N',$-di-n-hexyl-thio-diglycolamide (Crea), and N,N,N',N'-tetra-2-ethylhexyl-

(a) *N,N,N′,N′,N″,N″*-hexa-*n*-octylnitrilotriacetamide
(HONTA)

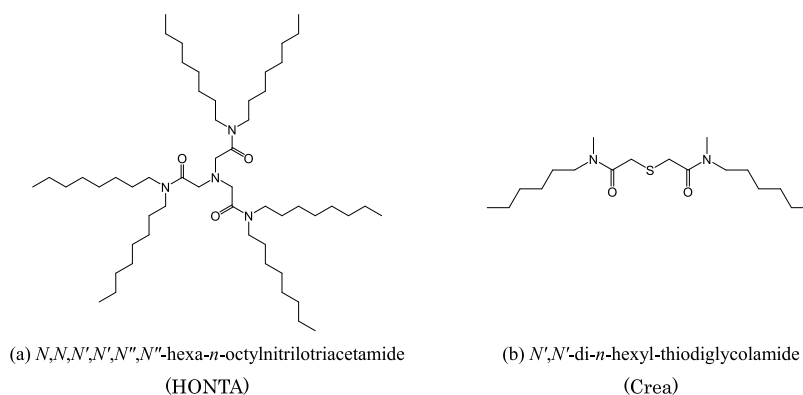(b) *N′,N′*-di-*n*-hexyl-thiodiglycolamide
(Crea)

Fig. 1. Molecular structures of extractants.

thiodiglycolamide (TEHTDGA) have shown good adsorption performance toward Pd(II) under nitric acid conditions same as solvent extractant [7–10]. Furthermore, it has been demonstrated that high adsorption capability is maintained despite degradation due to radiolysis concerning the adsorption performance under radiation circumstances, which must be taken into account for the recovery of metal ions from HLLW [11]. Another benefit of using impregnated silica-based adsorbent is that multiple extractants can be impregnated into SiO$_2$–P simultaneously. In the previous study, the synergistic effect of adsorption toward other metal ions was observed by combining Crea and 2,2′, 2″-nitrilotris[*N,N*-bis (2-ethylhexyl) acetamide] (TAMIA-EH), which has three amide groups in the structure [12]. Focusing on the adsorption of elements other than Pd(II), it has been reported that *N,N,N′,N′,N″, N″*-hexa-*n*-octylnitrilotriacetamide (HONTA), which has a similar structure to TAMIA-EH, is a promising extractant for the separation of Minor actinide [13,14].

For the effective recovery of platinum-group metals from HLLW, an impregnated silica-based adsorbent was prepared in this study by combining the HONTA extractant with three amide groups, the Crea extractant with two amide groups, and SiO$_2$–P. Then, through batch-adsorption and chromatographic separation experiments, the adsorption and separation performance of platinum-group metals on prepared (HONTA + Crea)/SiO$_2$–P adsorbent was evaluated along with co-existing metal ions in terms of the effect of HNO$_3$ concentration, contact time, reaction temperature, adsorption isotherm, γ-ray irradiation, and separation behavior.

2. Experimental

2.1. Materials

The newly synthesized adsorbent comprised SiO$_2$–P particle, HONTA extractant, and Crea extractant. The physical properties of SiO$_2$–P particles used as substrate were a diameter of 40–60 μm and a pore size of 50 nm [10]. The matrix of copolymer in SiO$_2$–P is the styrene–divinylbenzene. HONTA was synthesized following the reported procedure, and Crea (Creastar Pd-EX) was attained from Chemicrea Inc. (Tokyo, Japan) [15]. The structures of HONTA and Crea are shown in Fig. 1.

Simulated HLLW was reproduced by each reagent of 15 metal ions. These are the major metal ions produced by nuclear fission reaction and composition of actual HLLW, nitrate solution (Ru(III), Rh(III), and Pd (II)); nitrates (Zr(IV), Cs(I), Sr(II), Ba(II), La(III), Ce(III), Nd(III), Sm(III), Eu(III), and Gd(III)); molybdate (Mo(VI)); oxide (Re(VII)). The nitric acid solution composed of single metal ion Ru(III), Pd(II), or Re(VII) was used for the experiment of adsorption amount and isotherm. Concentrated nitric acid and deionized water were used to alter the nitric acid concentration of the simulated HLLW and the nitric acid solution

composed of a single metal ion following the experimental circumstances.

2.2. Synthesis of (HONTA + Crea)/SiO$_2$–P

A (HONTA + Crea)/SiO$_2$–P adsorbent was prepared by impregnating HONTA and Crea extractants into SiO$_2$–P particles following the previous study [9,16]. The synthesis procedure is as follows: First, SiO$_2$–P was washed with methanol to remove impurities. Second, the mixture of 10 g each of HONTA and Crea dissolved in dichloromethane and washed 20 g of SiO$_2$–P were stirred for 1 h at room temperature. Third, the dichloromethane was distilled under the pressure-reduced condition at 313 K to impregnate the extractant into SiO$_2$–P pores using a rotary evaporator. Then, (HONTA + Crea)/SiO$_2$–P adsorbent was obtained by vacuum drying at 313 K for over 12 h.

2.3. Experiments

The adsorption and separation performance of synthesized (HONTA + Crea)/SiO$_2$–P adsorbent was evaluated by batch-adsorption and chromatographic separation experiments using the simulated HLLW constituted by 5 mM (M = mol dm^{-3}) of 15 metal ions and the nitric acid solution composed of 5–100 mM of single metal ion. Although the metal ion concentration of actual HLLW alters based on the fission product yield, for each metal ion, the concentration of simulated HLLW was fixed to obtain the basic adsorption characteristics of the adsorbent. Batch-adsorption experiments were conducted to investigate the effect of HNO$_3$ concentration, contact time, reaction temperature, adsorption isotherm, and γ-ray irradiation on the adsorption performance. The condition of the batch-adsorption experiment was 20 cm^3 g^{-1} of the phase ratio, 4 cm^3 of simulated HLLW and 0.2 g of adsorbent, and 160 rpm of the stirring speed. For the investigation on the effect of the radiation, (HONTA + Crea)/SiO$_2$–P adsorbent was irradiated with γ-ray emitted from ^{60}Co in the ^{60}Co Gamma-ray Irradiation Facilities, Takasaki Advanced Radiation Research Institute, National Institute for Quantum Science and Technology (Chiba, Japan) [11]. The effect of radiolysis on the adsorption performance was evaluated using irradiated (HONTA + Crea)/SiO$_2$–P and simulated HLLW. In addition, the radiation stability of (HONTA + Crea)/SiO$_2$–P was evaluated by measuring the leaked carbon from the adsorbent when the mixture of adsorbent and 2 M HNO$_3$ under 1.5 (= 1.2 cm^3/0.8 g, corresponding to the chromatographic separation experiment condition) and 20 (= 4 cm^3/0.2 g, corresponding to the batch-adsorption experiment condition) cm^3 g^{-1} of the phase ratio was irradiated with γ-ray. The condition of the chromatographic separation experiment was 10 mm of the inner diameter of the column, 120 mm of bed height and 5.06 g of weight of adsorbent, 0.5 cm^3 min^{-1} of flow rate, and 298 K of the outer temperature of the column. In the chromatographic separation experiment, 5 cm^3 of
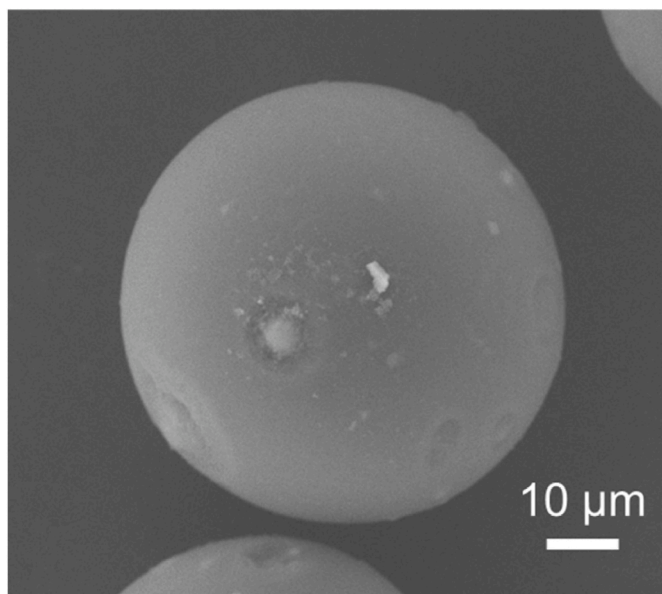
Fig. 2. SEM image of (HONTA + Crea)/SiO$_2$–P adsorbent.
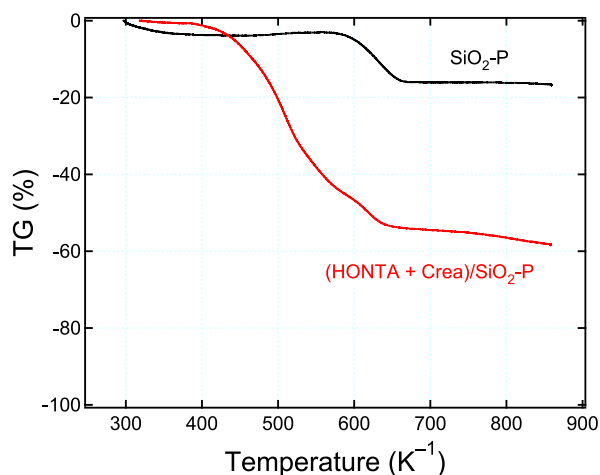

Fig. 3. Thermal gravimetric curves of (HONTA + Crea)/SiO$_2$–P.

Fig. 4. Effect of HNO$_3$ concentration on the adsorption of 15 metal ions onto (HONTA + Crea)/SiO$_2$–P. [Metal]: 5 mM for the 15 metal ions, [HNO$_3$]: from 0.1 to 6 M, temperature: 298 K, contact time: 5 h.

3. Results and discussion

3.1. Characterization

Fig. 2 shows the SEM image of (HONTA + Crea)/SiO$_2$–P adsorbent at a magnification of 1000 times. A particle of (HONTA + Crea)/SiO$_2$–P maintained the same spherical shape as the SiO$_2$–P without surface deposition, and the extractant was impregnated into the pores.

Fig. 3 shows the results of the thermal gravimetric curves of SiO$_2$–P and (HONTA + Crea)/SiO$_2$–P varying temperatures from room temperature to 850 K under the N$_2$ atmosphere. The composition ratio of extractant (HONTA and Crea) and SiO$_2$–P, containing 16.6 wt% of styrene–divinylbenzene, were 50.2 and 49.8 wt%, indicating that synthesis of (HONTA + Crea)/SiO$_2$–P adsorbent was conducted successfully because the thermal gravimetric results good agree with synthesis ratio.

3.2. Effect of HNO$_3$

The HLLW produced by the PUREX method is a nitric acid solution of about 2–3 M. Therefore, the adsorbent used to recover metal ions must be stable under nitric acid conditions. Fig. 4 shows the nitric acid concentration dependence of the distribution coefficient of 15 metal ions onto (HONTA + Crea)/SiO$_2$–P when the nitric acid concentration was varied from 0.1 to 6 M at 298 K under 5 h contact time in the batch-adsorption experiment. The distribution coefficient K_d (cm^3 g^{-1}) of each metal ion is described as follows:

$$K_d = \frac{C_0 - C_e}{C_e} \times \frac{V}{m}. \tag{1}$$

C_0 and C_e are the metal ion concentration at the initial time and equilibrium state (mM), respectively. V is the volume of simulated HLLW (cm^3). m is the amount of (HONTA + Crea)/SiO$_2$–P adsorbent (g). At the present HNO$_3$ condition, the distribution coefficients of Pd(II) adsorption on (HONTA + Crea)/SiO$_2$–P remained constant owing to the lower limit of determination in the ICP–AES measurement. (HONTA + Crea)/SiO$_2$–P adsorbent showed high adsorption performance of Pd(II) owing to the affinity between Pd(II) and sulfur donor of Crea extractant based on the HSAB theory [7]. Additionally, the nitrogen donor of the HONTA extractant, which is assumed to be an electron donor and behaving as a soft base donor, is expected to contribute to Pd(II) adsorption because of the charge interactions between Pd(II) and nitrogen donor [17–19]. For other metal ions, significant adsorption performance was observed toward Zr(IV) and Mo(VI). Compared with studies using impregnated silica-based adsorbents with Crea, the high

simulated HLLW constituted 5 mM of 15 metal ions as the feed solution, 30 cm^3 of 2 M HNO$_3$ as the washing solution, 30 cm^3 of 0.2 M thiourea in 0.1 M HNO$_3$ as the first eluent, 30 cm^3 of 5 M HNO$_3$ as the second eluent, and 50 cm^3 of 0.05 M diethylenetriamine pentaacetate acid (DTPA) and 0.5 M Na$_2$CO$_3$ solution as the third eluent was put into the column sequentially.

Surface observation and thermogravimetry of the adsorbent were conducted using scanning electron microscopy (SEM, TM3030Plus, Hitachi, Ltd., Tokyo, Japan) and a simultaneous differential thermal analysis and thermogravimetric apparatus (DTG-60, Shimadzu Corporation), respectively, for the characterization of the synthesized (HONTA + Crea)/SiO$_2$–P adsorbent. The metal ion concentration in the aqueous phase after the batch-adsorption experiment and the effluent of the chromatographic separation experiment were measured using an atomic absorption spectrometer (AAS, AA-6200, Shimadzu Corporation, Kyoto, Japan) for Cs and an inductively coupled plasma atomic-emission spectrometer (ICP-AES, ICPE-9000, Shimadzu Corporation) for other metal ions. Furthermore, the leaked carbon was measured using a total organic carbon (TOC) analyzer (TOC-V$_{SCN}$, Shimadzu Corporation).
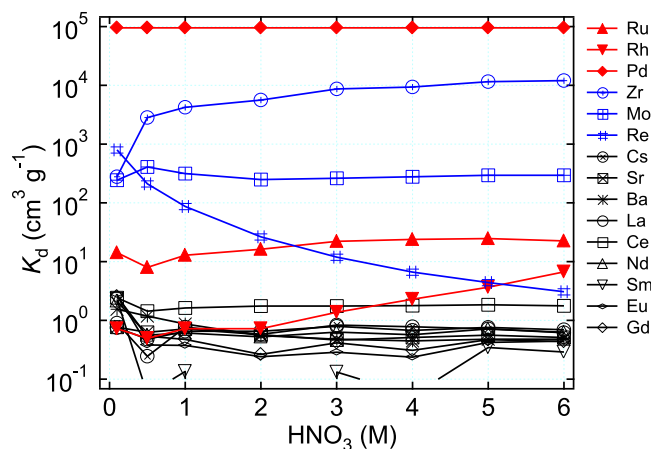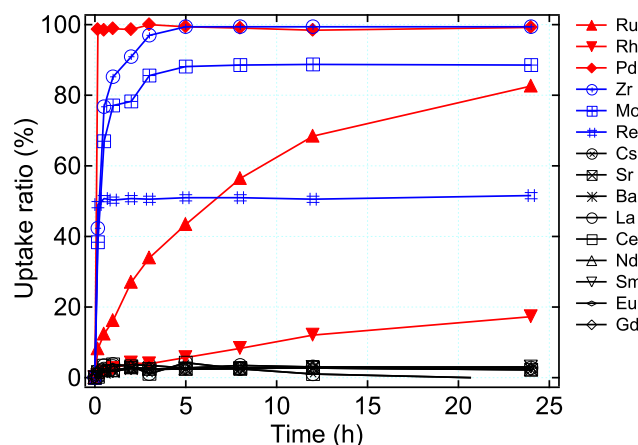
Fig. 5. Effect of contact time on the uptake ratio of 15 metal ions onto (HONTA + Crea)/SiO$_2$–P. [Metal]: 5 mM for the 15 metal ions, [HNO$_3$]: 2 M, temperature: 298 K, contact time: from 10 min to 24 h.
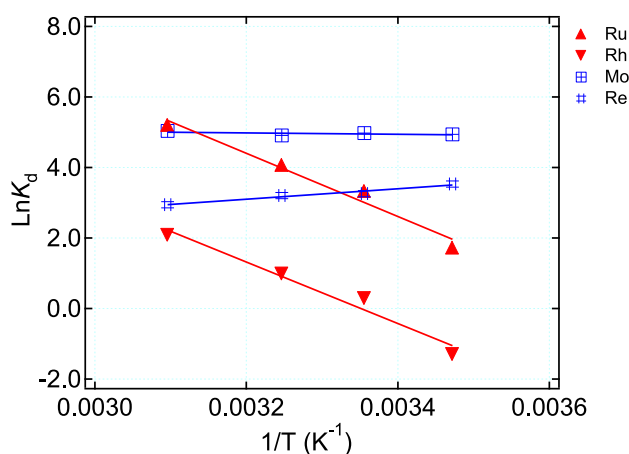

Fig. 6. Effect of reaction temperature on the distribution coefficient of Ru(III), Rh(III), Mo(VI), and Re(VII) onto (HONTA + Crea)/SiO$_2$–P. [Metal]: 5 mM for the 15 metal ions, [HNO$_3$]: 2 M, temperature: from 288 to 323 K, contact time: 5 h.

adsorption performance of Pd(II) was exhibited even when Crea was combined with HONTA. Those of Zr(IV) and Mo(VI) are considered due to being attributed to the HONTA because the distribution coefficients of Zr(IV) and Mo(VI) onto (Crea + TOA)/SiO$_2$–P and (Crea + dodeca-nol)/SiO$_2$–P without HONTA co-impregnated are less than 10^2.[10.20] At an HNO$_3$ concentration of 0.1–6 M, the Pd(II) distribution coefficient maintained above 10^4, indicating stable adsorption performance under nitric acid conditions.

3.3. Effect of contact time

The contact time dependence of adsorption was evaluated by changing the contact time from 10 min to 24 h in a batch-adsorption experiment. Fig. 5 shows the uptake ratio of 15 metal ions onto (HONTA + Crea)/SiO$_2$–P at 298 K under 2 M HNO$_3$ concentrations. The uptake ratio R (%) of each metal ion is described as follows:

$$R = \frac{C_0 - C_t}{C_0} \times 100. \tag{2}$$

C_t is the metal ion concentration at a particular time (mM). Almost all

Table 1
Values of the thermodynamic parameters for the adsorption of Ru(III), Rh(III), Mo(VI), and Re(VII) onto (HONTA + Crea)/SiO$_2$–P.

	Ru(III)	Rh(III)	Mo(VI)	Re(VII)
ΔG^0 (kJ mol^{-1})				
288 K	−4.7	2.5	−11.8	−8.4
298 K	−7.5	0.1	−12.3	−8.3
308 K	−10.2	−2.3	−12.7	−8.1
323 K	−14.3	−6.0	−13.4	−7.9
ΔH^0 (kJ mol^{-1})	74.5	72.4	1.6	−12.3
ΔS^0 (kJ mol^{-1} K^{-1})	0.28	0.24	0.05	−0.01

Pd(II) was adsorbed within 10 min while Re(VII) adsorption reached an equilibrium state at an uptake ratio of about 50%. These tendencies indicate that the adsorption of Pd(II) and Re(VII) onto (HONTA + Crea)/SiO$_2$–P was very quick and well agreed with the results of other TDGA-type impregnated silica-based adsorbents [8–10,12,14,20]. The adsorption rate was in the order of Pd(II) and Re(VII) > Zr(IV) and Mo (VI) > Ru(III) > Rh(III), and the adsorption of Ru(III) and Rh(III) could not attain equilibrium at a contact time of 24 h. The high uptake ratio and rapid adsorption of Zr(IV) and Mo(VI) onto (HONTA + Crea)/SiO$_2$–P complements the result of the previous study, which described that the synergistic effect on adsorption of Zr(IV) and Mo(VI) by combining Crea and TAMIA-EH, which is one of the extractants with three amide groups in the structure, in case of using HONTA instead of TAMIA-EH in this study [12].

3.4. Effect of temperature

Fig. 6 shows the van 't Hoff plot indicating the relationship between the distribution coefficient and reaction temperature of Ru(III), Rh(III), Mo(VI), and Re(VII) adsorption. The experiments were performed using simulated HLLW containing 15 metal ions under 2 M HNO$_3$, 5 h contact time, and varying temperatures from 288 to 323 K. The thermodynamic parameters of adsorption calculated from the van 't Hoff equation and the Gibbs free energy equation were summarized in Table 1. Here, these equations[21,22] are described as follows:

$$\ln K_d = -\frac{\Delta H^0}{R_u T} + \frac{\Delta S^0}{R_u}, \tag{3}$$

$$\Delta G^0 = \Delta H^0 - \Delta S^0 T. \tag{4}$$

ΔH^0 and ΔG^0 are the changes in enthalpy and the Gibbs free energy (kJ mol^{-1}). R_u is the universal gas constant (= 8.314×10^{-3} kJ mol^{-1} K^{-1}). ΔS^0 is the changes in the entropy (kJ mol^{-1} K^{-1}). T is the reaction temperature (K). Since (HONTA + Crea)/SiO$_2$–P has high adsorption performance toward Pd(II) and the effect of temperature on Pd(II) adsorption does not appear clearly, the result for Pd(II) are omitted in Fig. 6 and Table 1. The relationship between ln(K_d) and T^{-1} of Ru(III), Rh(III), Mo(VI), and Re(VII) adsorption is not discontinuous but almost linear, demonstrating stable adsorption performance for temperature. From the thermodynamic parameters, the ΔH^0 value of Ru(III) and Rh (III) adsorption was positive, which means the adsorption is an endo-thermic reaction. Adsorption of Ru(III) and Rh(III) are also more sensitive to reaction temperature than those of Mo(VI) and Re(VII). High-temperature conditions are preferable when these four metal ions are simultaneously adsorbed. The negative ΔG^0 value of Ru(III), Mo(VI), and Re(VII) adsorption indicates the reaction proceeding spontaneously under the present temperature conditions.

3.5. Adsorption amount and isotherm

In the previous study, since the adsorption of Pd(II) by the TDGA-type adsorbent showed a high correlation with the Langmuir isotherm model, the adsorption amount and isotherm of (HONTA + Crea)/SiO$_2$–P were also evaluated using the Langmuir isotherm model in this study
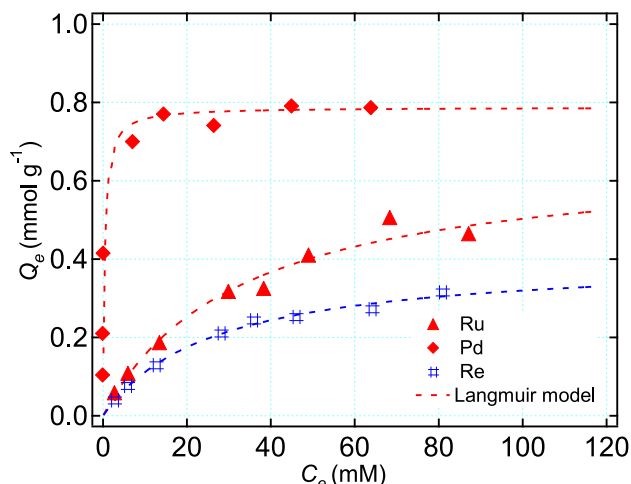
Fig. 7. Adsorption isotherm of Ru(III), Pd(II), and Re(VII) onto (HONTA + Crea)/SiO$_2$–P. [Metal]: from 5 to 100 mM, [HNO$_3$]: 2 M, temperature: 298 K, contact time: 5 h.

Table 2
Langmuir isotherm parameters for the adsorption of Ru(III), Pd(II), and Re(VII) onto (HONTA + Crea)/SiO$_2$–P.

Metal ions	Q_m (mmol g^{-1})	K_L (L mmol^{-1})	R^2
Ru(III)	0.67	0.03	0.966
Pd(II)	0.79	2.53	0.999
Re(VII)	0.40	0.04	0.992

[8–10,12,14,20]. The Langmuir isotherm model is [23,24]described as follows:

$$Q_e = \frac{Q_m K_L C_e}{1 + K_L C_e} \quad \text{(nonlinear)}, \tag{5}$$

$$\frac{C_e}{Q_e} = \frac{1}{Q_m} C_e + \frac{1}{Q_m K_L} \quad \text{(linear)}. \tag{6}$$

Q_e and Q_m are the adsorbed amount of each metal ion at the equilibrium state, and the theoretical maximum adsorbed amount by the Langmuir isotherm model (mmol g^{-1}), respectively. K_L is the model parameter of the Langmuir isotherm model (L mmol^{-1}). Fig. 7 shows the adsorption amounts and fitting curves calculated by the Langmuir isotherm model toward Ru(III), Pd(II), and Re(VII) adsorption. Calculated parameters by the Langmuir isotherm model of three metal ions are summarized in Table 2. The adsorbed amount of Pd(II) reached an equilibrium state at about 0.79 mmol g^{-1}, while those of Ru(III) and Re(VII) could not. The correlation coefficients between experimental results and the Langmuir isotherm model were well fitted with above 0.96, indicating that the adsorption of Ru(III), Pd(II), and Re(VII) was considered as single layer adsorption on (HONTA + Crea)/SiO$_2$–P. The order of theoretical maximum adsorbed amounts was Pd(II) > Ru(III) > Re(VII), indicating (HONTA + Crea)/SiO$_2$–P has sufficient adsorption performance for Pd(II).

3.6. Effect of γ-ray irradiation

In the assumed separation process using extraction chromatography, the adsorbent is in direct contact with the HLLW and is therefore considerably affected by radiation. Gamma-ray irradiation mainly leads to a degradation of the adsorption performance due to radiolysis of the extractant as inorganic support SiO$_2$ has mechanical strength and radiation resistance. Therefore, the radiation effect on the extractant in the
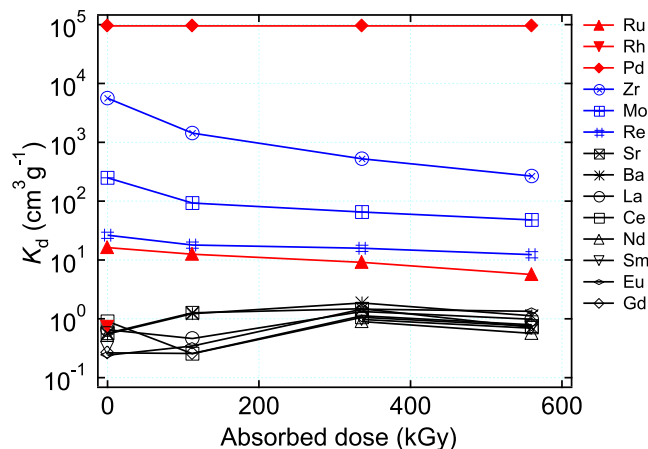

Fig. 8. Effect of γ-ray irradiation on the distribution coefficient of 15 metal ions onto (HONTA + Crea)/SiO$_2$–P at 298 K. [Metal]: 5 mM for the 15 metal ions, [HNO$_3$]: 2 M, temperature: 298 K, contact time: 5 h.

adsorbent must be estimated. The absorbed dose D of the adsorbent in the chromatographic separation condition was roughly estimated as 7.7 kGy h^{-1} using the following equation.

$$D = \frac{D_{HLLW}}{W_{ad} + W_{HLLW}} = \frac{E_{HLLW} \times V_{HLLW}}{W_{ad} + (\rho_{HLLW} \times V_{HLLW})} = \frac{E_{HLLW} \times V_{col} \times \varepsilon_{col}}{W_{ad} + (\rho_{HLLW} \times V_{col} \times \varepsilon_{col})}. \tag{7}$$

Here, D is the absorbed dose (Gy h^{-1}), D_{HLLW} is the dose rate of HLLW in the column (J h^{-1}), W_{ad} and W_{HLLW} are the weights (kg) of the adsorbent and HLLW in the column, respectively, E_{HLLW} is the emitting energy from the elements included in the HLLW calculated from the calorific value composition of nuclear-spent fuel of 45 GWd tHM^{-1} after a 5-year cooling period when 500 m^3 of HLLW was produced from 1 tHM of nuclear-spent fuel (1.79 × 10^4 J h^{-1} L^{-1}) [25], V_{col} and V_{HLLW} are the volumes (L) of the column and HLLW, respectively, ε_{col} is the porosity (assumed to be 0.5), and ρ_{HLLW} is the density of HLLW (assumed to be 1.26 kg L^{-1}) [25]. Furthermore, we conservatively assumed that all of the emitting energy is absorbed by the adsorbent and HLLW in the column. The value of 560 kGy corresponds to the condition, where the adsorbent is in contact with HLLW for 72 h. In the actual process, U and Pu are separated by the PUREX process in advance, and heat-generating metals, such as Cs and Sr, can also be separated using the extraction chromatography method at a previous stage [26]. Hence, the radiation dose affecting the adsorbent at the stage of PGMs separation is substantially lower than the estimated absorbed dose [27].

The extractants are known to produce several degradation products under the influence of irradiation. Based on the analysis of radiolytic degradation products using TEHTDGA extractant, which is one of the TDGA-type extractants, it is expected that the amide bond, thioether bond, and carboxyl linkage of the amide in the structure of Crea and HONTA are cleaved by γ-ray irradiation [27].

Fig. 8 shows the effect of radiolysis of the impregnated extractant on the adsorption performance of 15 metal ions onto preirradiated (HONTA + Crea)/SiO$_2$–P at 298 K under 2 M HNO$_3$ concentration and 5 h contact time. The distribution coefficients of Ru(III), Zr(IV), Mo(VI), and Re(VII) were gradually decreased with increasing absorbed dose up to 560 kGy, indicating the deterioration of adsorption performance was caused by the radiolysis of the extractant. However, (HONTA + Crea)/SiO$_2$–P shows high adsorption performance toward Pd(II) ($K_d > 10^4$) because of the presence of a sufficient number of adsorption sites for Pd(II) on the adsorbent, as indicated by the results of the adsorption amount and isotherm (Fig. 7).
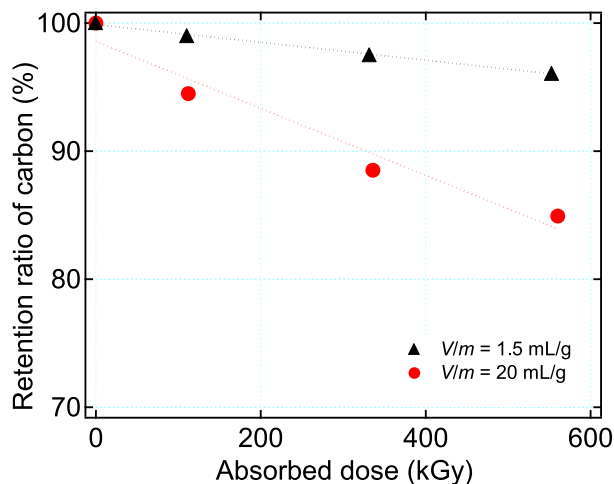
Then, the retention ratio of carbon in (HONTA + Crea)/SiO$_2$–P was

Fig. 9. Retention ratio of carbon in (HONTA + Crea)/SiO₂–P after γ-ray irradiation contacting with HNO₃ solution.
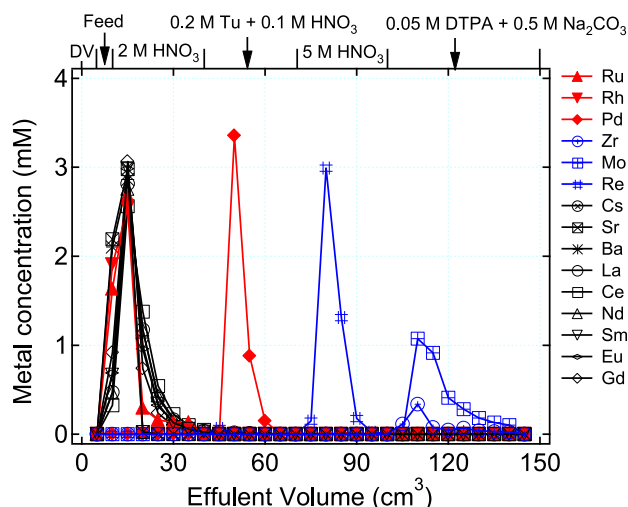

Fig. 10. Chromatographic separation results for 15 metal ions using (HONTA + Crea)/SiO₂–P. Flow rate: 0.5 cm³ min⁻¹, bed height: 120 mm, an inner diameter of the column: 10 mm, and temperature: 298 K. (Tu: Thiourea, DTPA: diethylenetriamine pentaacetate acid).

obtained by measuring the amount of leaked carbon from adsorbent to 2 M HNO₃ under γ-ray irradiation was shown in Fig. 9. The retention ratio R_C (%) is described as follows[11]:

$$R_C = \left(1 - \frac{C_{TOC}}{C_{AC}}\right) \times \frac{V}{m} \times 100. \tag{8}$$

C_{TOC} and C_{AC} are the concentration of dissolved carbon in the nitric acid solution (mg dm⁻³) and the amount of carbon loaded into the adsorbent (mg g⁻¹), respectively. The radiolysis of extractant into (HONTA + Crea)/SiO₂–P was observed due to the increased carbon leakage with increasing the absorbed dose by γ-ray irradiation. The deterioration of adsorbent under 20 cm³ g⁻¹ of phase ratio shows about 2.9 times greater than those under 1.5 cm³ g⁻¹, indicating the effect of radiolysis differs depending on the phase ratio.

3.7. Chromatography experiment

In the case of recovering metal ions from HLLW, adsorption and separation by column chromatography are effective in reducing the equipment configuration. Fig. 10 shows the chromatographic properties of (HONTA + Crea)/SiO₂–P using simulated HLLW. First, Pd(II), Zr(IV), Mo(VI), and Re(VII) were completely adsorbed onto (HONTA + Crea)/SiO₂–P from the feed solution. Then, 85% of Pd(II) and 96% of Re(VII) were recovered by 0.2 M thiourea in 0.1 M HNO₃ and 5 M HNO₃, respectively, while 85% of Zr(IV) and 40% of Mo(VI) remained on the column in case of using 0.05 M DTPA–0.5 M Na₂CO₃ solution.

4. Conclusions

An impregnated silica-based adsorbent was successfully prepared by impregnating HONTA and Crea extractants into SiO₂–P particles. The results of batch-adsorption experiments showed the high adsorption capability of (HONTA + Crea)/SiO₂–P toward Pd(II). This adsorbent also demonstrated those toward Zr(IV) and Mo(VI) by combining Crea with HONTA. The adsorption of Ru(III), Rh(III), Mo(VI), and Re(VII) showed stable adsorption with respect to temperature because the results showed a continuous linear change at the temperature from 288 to 323 K. From the results of isotherm analysis using Langmuir isotherm model, the adsorption of Ru(III), Pd(II), and Re(VII) onto (HONTA + Crea)/SiO₂–P were classified as single layer adsorption. The adsorption performance decreased, and the adsorbent deterioration was observed due to γ-ray irradiation. However, the adsorption capability of Pd(II) onto (HONTA + Crea)/SiO₂–P remained high in the case of the absorbed dose of up to about 560 kGy. The preferred adsorption and separation tendency of Pd(II) was shown in a chromatographic separation experiment using 0.2 M thiourea in 0.1 M HNO₃ as eluent. Additionally, the possibility of obtaining Zr(IV), Mo(VI), and Re(VII) using the (HONTA + Crea)/SiO₂–P adsorbent was observed.

Declaration of competing interest

The authors declare that they have no known competing financial interests or personal relationships that could have appeared to influence the work reported in this paper.

Nomenclature

C_0	Metal ion concentration at the initial time (mM)
C_{AC}	Amount of carbon loaded into the adsorbent (mg g⁻¹)
C_e	Metal ion concentration at equilibrium state (mM)
C_t	Metal ion concentration at a certain time (mM)
C_{TOC}	Concentration of dissolved carbon in the nitric acid solution (mg dm⁻³)
D	Absorbed dose (Gy h⁻¹)
D_{HLLW}	Dose rate of HLLW in the column (J h⁻¹)
E_{HLLW}	Emitting energy from the elements included in the HLLW (J h⁻¹ L⁻¹)
K_d	Distribution coefficient (cm³ g⁻¹)
K_L:	Model parameter of the Langmuir isotherm model (L mmol⁻¹)
m	Weight of the adsorbent (g)
R	Uptake ratio (%)
R_C	Retention ratio (%)
R_u	Universal gas constant (kJ mol⁻¹ K⁻¹)
Q_e	Adsorbed amount of metal ion at equilibrium state (mmol g⁻¹)
Q_m	Theoretical maximum adsorbed amount by the Langmuir isotherm model (mmol g⁻¹)
T	Reaction temperature (K)
V	Volume of simulated HLLW (cm³)

V_{col}	Volume of the column (L)
V_{HLLW}	Volume of HLLW in the column (L)
W_{ad}	Weight of adsorbent in the column (kg)
W_{HLLW}	Weight of HLLW in the column (kg)
ΔH^0	Changes in enthalpy (kJ mol^{-1})
ΔG^0	Changes in the Gibbs free energy (kJ mol^{-1})
ΔS^0	Changes in the entropy (kJ mol^{-1} K^{-1})
ε_{col}	Porosity (−)
ρ_{HLLW}	Density of the HLLW (kg L^{-1})

References

[1] IAEA, Techniques for the Solidification of High-Level Wastes, IAEA Technical Reports Series, 1997, p. 176.

[2] L. Rodriguez-Penalonga, B.Y.M. Soria, A review of the nuclear fuel cycle strategies and the spent nuclear fuel management technologies, Energies 10 (2017) 1235, https://doi.org/10.3390/en10081235.

[3] C. Krause, B. Luckscheiter, Properties and behavior of the platinum group metals in the glass resulting from the vitrification of simulated nuclear fuel reprocessing waste, J. Mater. Res. 6 (1991) 2535–2546, https://doi.org/10.1557/JMR.1991.2535.

[4] Z. Kolarik, E.V. Renard, Recovery of value fission platinoids from spent nuclear fuel part I: general considerations and basic chemistry, Platin. Met. Rev. 47 (2003) 74–87.

[5] K. Shimojo, Solvent extraction in analytical separation techniques, Anal. Sci. 34 (2018) 1345–1346, https://doi.org/10.2116/analsci.highlights1812.

[6] A. Zhang, Y. Wei, M. Kumagai, Y. Koma, A new partitioning process for high-level liquid waste by extraction chromatography using silica-substrate chelating agent impregnated adsorbents, J. Alloys Compd. 390 (2005) 275–281, https://doi.org/10.1016/j.jallcom.2004.08.034.

[7] R.G. Pearson, Hard and soft acids and bases, J. Am. Chem. Soc. 85 (1963) 3533–3539, https://doi.org/10.1021/ja00905a001.

[8] T. Ito, S.-Y. Kim, Y. Xu, K. Hitomi, K. Ishii, R. Nagaishi, T. Kimura, Adsorption behavior of platinum group metals in simulated high level liquid waste using macroporous (MOTDGA-TOA)/SiO$_2$-P silica-based absorbent, Separ. Sci. Technol. 48 (2013) 2616–2625, https://doi.org/10.1080/01496395.2013.807290.

[9] N. Osawa, M. Kubota, H. Wu, S.-Y. Kim, Development of *N,N,N′,N′*-tetra-2-ethylhexyl-thiodiglycolamide silica-based adsorbent to separate useful metals from simulated high-level liquid waste, J. Chromatogr. A 1678 (2022), 463353, https://doi.org/10.1016/j.chroma.2022.463353.

[10] Y. Xu, S.-Y. Kim, T. Ito, T. Tada, K. Hitomi, K. Ishii, Adsorption properties and behavior of the platinum group metals onto a silica-based (Crea + TOA)/SiO$_2$-P adsorbent from simulated high level liquid waste of PUREX reprocessing, J. Radioanal. Nucl. Chem. 297 (2013) 41–48, https://doi.org/10.1007/s10967-012-2314-9.

[11] T. Ito, S.-Y. Kim, N. Nagano, K. Hitomi, Effect of γ-ray irradiation on thiodiglycolamide-type extractant-impregnated adsorbents for separation of platinum group metals from high-level liquid waste, Energy Proc. 131 (2017) 195–202, https://doi.org/10.1016/j.egypro.2017.09.427.

[12] H. Wu, S.-Y. Kim, M. Miwa, S. Matsuyama, Synergistic adsorption behavior of a silica-based adsorbent toward palladium, molybdenum, and zirconium from simulated high-level liquid waste, J. Hazard Mater. 411 (2021), 125136, https://doi.org/10.1016/j.jhazmat.2021.125136.

[13] Y. Sasaki, Y. Tsubata, Y. Kitatsuji, Y. Morita, Novel soft-hard donor ligand, NTAamide, for mutual separation of trivalent actinoids and lanthanoids, Chem. Lett. 42 (2013) 91–92, https://doi.org/10.1246/cl.2013.91.

[14] Y. Ban, H. Suzuki, S. Hotoku, N. Tsutsui, Y. Tsubata, T. Matsumura, Minor actinides separation by *N,N,N′,N′,N″,N″*-hexaoctyl nitrilotriacetamide (HONTA) using mixer-settler extractors in a hot cell, Solvent Extr. Ion Exch. 37 (2019) 489–499, https://doi.org/10.1080/07366299.2019.1693486.

[15] T. Akuzawa, S.-Y. Kim, M. Kubota, H. Wu, S. Watanabe, Y. Sano, M. Takeuchi, T. Arai, Design of MA(III)/Ln(III) separation process of extraction chromatography technology, J. Radioanal. Nucl. Chem. 331 (2022) 5851–5858, https://doi.org/10.1007/s10967-022-08658-7.

[16] N. Osawa, M. Kubota, H. Wu, S.-Y. Kim, Adsorption and separation behavior of Pd (II) from simulated high-level liquid waste using *N,N,N′,N′*-tetra-2-ethylhexyl-thiodiglycolamide silica-based adsorbent, Separ. Sci. Technol. 57 (2022) 48–59, https://doi.org/10.1080/01496395.2021.1883653.

[17] S. Xu, S. Ning, Y. Wang, X. Wang, H. Dong, L. Chen, X. Yin, T. Fujita, Y. Wei, Precise separation and efficient enrichment of palladium from wastewater by amino-functionalized silica adsorbent, J. Clean. Prod. 396 (2023), 136479, https://doi.org/10.1016/j.jclepro.2023.136479.

[18] S. Ning, S. Zhang, W. Zhang, J. Zhou, S. Wang, X. Wang, Y. Wei, Separation and recovery of Rh, Ru and Pd from nitrate solution with a silica-based *Iso*Bu-BTP/SiO$_2$-P adsorbent, Hydrometallurgy 191 (2020), 105207, https://doi.org/10.1016/j.hydromet.2019.105207.

[19] S.-C. Zhang, S.-Y. Ning, J. Zhou, S.-Y. Wang, W. Zhang, X.-P. Wang, Y.-Z. Wei, New insight into the adsorption of ruthenium, rhodium, and palladium from nitric acid solution by a silica-polymer adsorbent, Nucl. Sci. Tech. 31 (2020) 34, https://doi.org/10.1007/s41365-020-0744-6.

[20] Y. Xu, S.-Y. Kim, T. Ito, H. Tokuda, K. Hitomi, K. Ishii, Adsorption behavior of platinum group metals onto a silica-based (Crea + Dodec)/SiO$_2$-P extraction resin from simulated high level liquid waste, Separ. Sci. Technol. 50 (2015) 260–266, https://doi.org/10.1080/01496395.2014.956222.

[21] M. Naushad, Z.A. Alothman, Md R. Awual, M.M. Alam, G.E. Eldesoky, Adsorption kinetics, isotherms, and thermodynamic studies for the adsorption of Pb^{2+} and Hg^{2+} metal ions from aqueous medium using Ti(IV) iodovanadate cation exchanger, Ionics 21 (2015) 2237–2245, https://doi.org/10.1007/s11581-015-1401-7.

[22] E.C. Lima, A. Hosseini-Bandegharaei, J. Carlos Moreno-Piraján, I. Anastopoulos, A critical review of the estimation of the thermodynamic parameters on adsorption equilibria. Wrong use of equilibrium constant in the Van 't Hoof equation for calculation of thermodynamic parameters of adsorption, J. Mol. Liq. 273 (2019) 425–434, https://doi.org/10.1016/j.molliq.2018.10.048.

[23] T.S. Khayyun, A.H. Mseer, Comparison of the experimental results with the Langmuir and Freundlich models for copper removal on limestone adsorbent, Appl. Water Sci. 9 (2019) 170, https://doi.org/10.1007/s13201-019-1061-2.

[24] M.C. Ncibi, Applicability of some statistical tools to predict optimum adsorption isotherm after linear and non-linear regression analysis, J. Hazard Mater. 153 (2008) 207–212, https://doi.org/10.1016/j.jhazmat.2007.08.038.

[25] JAEA, Handbook on Process and Chemistry of Nuclear Fuel Reprocessing, third ed., 2015, https://doi.org/10.11484/jaea-review-2015-002. JAEA-Review 2015-002.

[26] S.-Y. Kim, Y. Xu, T. Ito, Y. Wu, T. Tada, K. Hitomi, E. Kuraoka, K. Ishii, A novel partitioning process for treatment of high level liquid waste using macroporous silica-based adsorbents, J. Radioanal. Nucl. Chem. 295 (2013) 1043–1050, https://doi.org/10.1007/s10967-012-1878-8.

[27] R. Ruhela, J.N. Sharma, B.S. Tomar, K.K. Singh, M. Kumar, P.N. Bajaj, R.C. Hubli, A.K. Suri, Studies on hydrolytic and radiolytic stability of *N,N,N′,N′*-tetra-(2-ethylhexyl) thiodiglycolamide T(2EH)TDGA, Radiochim. Acta 100 (2012) 37–44, https://doi.org/10.1524/ract.2011.1892.